

Laboratory-based GEMTIP analysis of spectral IP data for mineral discrimination

Michael S. Zhdanov, Vladimir Burtman*, University of Utah and TechnoImaging, Masashi Endo and Glenn A. Wilson, TechnoImaging

Summary

The generalized effective medium theory for induced polarization (GEMTIP) enables one to model and invert the complex resistivity (CR) spectra for rock and fluid parameters such as matrix resistivity, grain size, grain resistivity, fraction volumes, porosity, fluid saturations, and polarizability. Moreover, GEMTIP can explain anisotropic resistivity in terms of grain orientation. In this work, the GEMTIP model is used to invert laboratory-based complex resistivity measurements for the aforementioned rock and fluid properties. We have applied the GEMTIP model to analyze the IP phenomena in both mineralized rocks, and hydrocarbon-bearing reservoir rocks. From laboratory measurements of mineralized rock samples, we show how the mineral properties recovered from GEMTIP analyses of CR spectra can be correlated with optical microscopy, QEMScan and x-ray tomographic mineralogical analyses.

Introduction

The premise of the various induced polarization (IP) methods is that minerals (particularly sulfides) may be discriminated from the interpretation of electromagnetic (EM) survey data. This can be realized since the effective conductivity is frequency dependent, and most often explained in terms of physico-chemical polarization effects of mineralized particles and/or by electrokinetic effects in pore spaces (e.g., Wait, 1959; Marshall and Madden, 1959; Luo and Zhang, 1998). The most popular effective conductivity model used for interpreting IP data is the Cole-Cole relaxation model (Pelton et al., 1978) whereby the various relaxation parameters are empirically determined from laboratory experiments. Wait (1983) introduced a relaxation model based on conductive spheres in a uniform matrix.

Until recently, there remained an absence of a comprehensive rock physics model that could relate actual rock and fluid properties (such as mineral fraction volume, grain size, grain shape, conductivity, polarizability, porosity, and fluid saturation) to CR spectra and/or observed EM data. To this end, the generalized effective medium theory for induced polarization (GEMTIP) (Zhdanov, 2008) was developed as a unified method of directly relating rock and fluid properties to a CR spectrum for the equivalent multi-phase medium. Moreover, GEMTIP can explain macroscopic anisotropic resistivity in terms of microscopic grain orientation. Over the years, GEMTIP has been applied to analyze the IP phenomena in both mineralized rocks and hydrocarbon-bearing reservoir

rocks (e.g., Emond et al., 2006; Zhdanov et al., 2008; Zhdanov and Burtman, 2009; Burtman et al., 2010, 2011). In this paper, we provide examples where GEMTIP has been used to model and invert laboratory-measured CR spectra for the rock samples that have been independently analyzed for their mineralogical composition using optical microscopy, QEMScan and x-ray tomographic mineralogical analyses. This enables us to potentially better understand the IP mechanisms of different types of mineralized rocks.

Generalized effective medium theory of induced polarization (GEMTIP)

IP modelling and inversion is usually based on 2D or 3D models populated with electrical properties from which the complex conductivity, $\hat{\sigma}$, may be calculated. This complex conductivity is that of an effective medium.

$$\rho_{ef} = \rho_0 \left\{ 1 + \sum_{i=1}^N \left\{ f_i m_i \left\{ 1 - \frac{1}{1 + \{-i\omega\tau_i\}^{C_i}} \right\} \right\} \right\}^{-1}$$

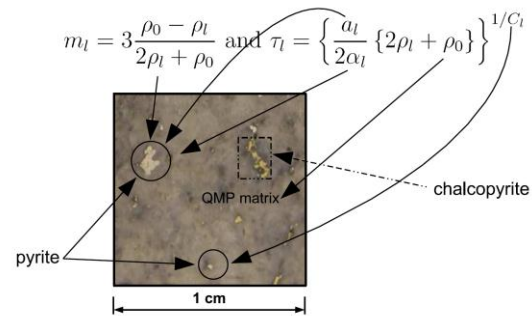


Figure 1. An example of the application of GEMTIP to a mineral rock sample defined with two different types of spherical inclusions (pyrite and chalcopyrite) embedded in a uniform matrix (quartz monzonite porphyry, QMP).

More formally, the effective conductivity, $\hat{\sigma}_e$, of a generally heterogeneous medium is defined from the current density, \mathbf{J}_e , in an effective medium which is equal to the average current density as would be measured in the original, heterogeneous medium:

$$\mathbf{J}_e = \hat{\sigma}_e \cdot \langle \mathbf{E} \rangle = \langle \hat{\sigma} \cdot \mathbf{E} \rangle, \quad (1)$$

where $\langle \dots \rangle$ denotes volume average, and the conductivity, $\hat{\sigma}$, may be anisotropic and frequency dependent. Zhdanov (2008) formally introduced GEMTIP as being based on

Laboratory-based GEMTIP analysis of spectral IP data

Maxwell's equations, and can predict the frequency-dependent and anisotropic effective conductivity of a medium characterized with parameters directly related to the rock properties, i.e., fraction volume, grain size, grain shape, conductivity, polarizability, porosity, and fluid saturation:

$$\hat{\sigma}_e = \hat{\sigma}_0 + \sum_{l=1}^N [\hat{\mathbf{I}} + \hat{\mathbf{p}}]^{-1} [\hat{\mathbf{I}} - \Delta\hat{\sigma}_l^p \hat{\Gamma}_l]^{-1} [\hat{\mathbf{I}} + \hat{\mathbf{p}}_l] \Delta\hat{\sigma}_l f, \quad (2)$$

where $\Delta\hat{\sigma}_l$ is the anomalous conductivity tensor, $\hat{\mathbf{p}}$ is the polarizability tensor:

$$\hat{\mathbf{p}} = [\hat{\mathbf{I}} + \hat{\mathbf{p}}]^{-1} \Delta\hat{\sigma}_l, \quad (3)$$

$\hat{\mathbf{p}}_l$ is the surface polarizability tensor, $\hat{\Gamma}_l$ is the volume depolarization tensor, and the index l corresponds to the grain type. In general, each grain type may take a different ellipticity (e.g., Figure 2) and orientation. It can be shown that the effective conductivity is anisotropic if the grains are oriented in the same direction, and is isotropic if the grains are all randomly oriented.

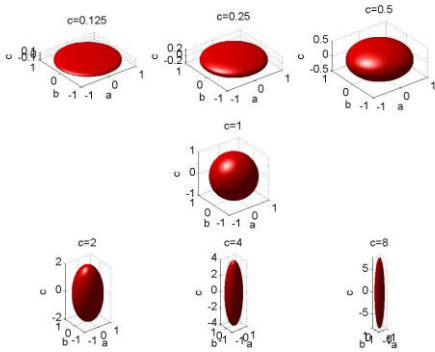


Figure 2. Example of the ellipticity of different grain types.

As an example of the form GEMTIP can assume, we may consider a multiphase composite polarized medium with two different types of spherical inclusions. Following Zhdanov (2008), equation (2) can be reduced to the form:

$$\tilde{\rho} = \rho_0 \left\{ 1 + \sum_{l=1}^N \left\{ f_l m_l \left\{ 1 - \frac{1}{1 + (-i\omega\tau_l)c_l} \right\} \right\} \right\}^{-1}, \quad (2)$$

where ρ_0 is the matrix resistivity, f_l is the fraction volume of the l mineral, τ_l and c_l are the time and relaxation constants of the l mineral, and where:

$$m_l = 3 \frac{\rho_0 - \rho_l}{2\rho_l + \rho_0}, \quad (3)$$

where ρ_l is the resistivity of the l mineral.

GEMTIP modeling and inversion of CR spectra

As our first example of GEMTIP's application, Ostrander and Zong (1978) measured the CR spectra of artificial rocks containing different pyrite and chalcopyrite grain sizes, from 0.01 Hz to 110 Hz. As shown in Figure 3, GEMTIP is able to accurately replicate the IP peak of Ostrander and Zong's experimental work.

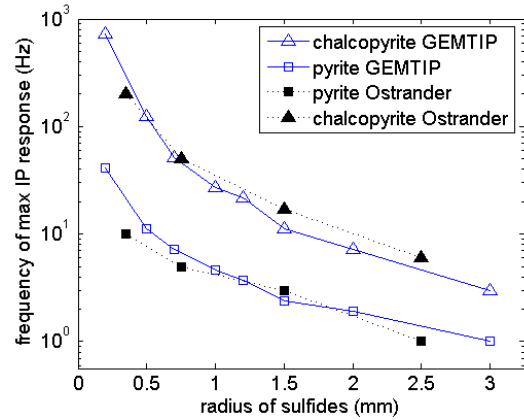


Figure 3. Comparison of GEMTIP modeling (blue) and experimental work by Ostrander and Zong (1978) for synthetic rocks containing pyrite and chalcopyrite of different grain sizes.

Next, we consider a quartz monzonite porphyry (QMP) sample from the Korri Kollo deposit in Bolivia, with a 15% pyrite fraction volume in a sericite and quartz matrix (Figure 4). The grain sizes average about 2 mm, but as shown in the x-ray tomography of Figure 4, are generally elongated.

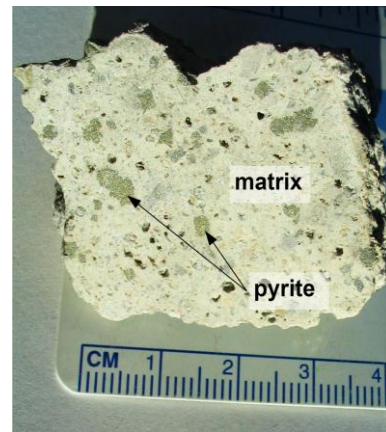


Figure 4. QMP sample with sericite and quartz matrix and pyrite inclusions shown.

Laboratory-based GEMTIP analysis of spectral IP data

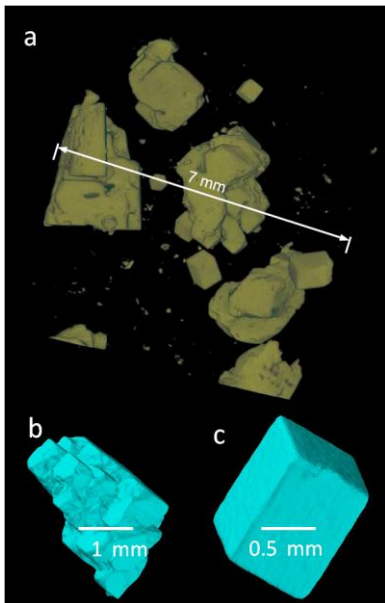


Figure 5. (a) X-ray tomographic image of the QMP sample. The image has been optimized to show the pyrite grains, with (b) and (c) being zoomed images of individual grains.

The GEMTIP-based effective conductivity is based on an analytic form. This means the Fréchet derivatives can be derived analytically. Any regularized inversion method (e.g., Zhdanov, 2002) can then be applied to invert observed CR spectra for the desired GEMTIP parameters. Using this approach, the measured CR spectra of the QMP sample were inverted (Figure 6) for several GEMTIP parameters which are detailed in Table 1. As expected, the GEMTIP model with elliptical grains achieved a lower misfit and more closely recovered the pyrite fraction volume the GEMTIP model with spherical grains.

Variable	Spherical GEMTIP	Elliptical GEMTIP
f_{pyrite}	12.03	12.03
C	0.72	0.72
r	2.5	-
r_x	-	2.5
r_y	-	2.5
r_z	-	5.0
α	0.8	0.8
Misfit	1.4	0.2

Table 1. Comparison of spherical and elliptical GEMTIP inversions for CR data for the QMP sample. Note that the same pyrite fraction volume was recovered. The ability to vary the grain dimensions enabled the elliptical GEMTIP model to achieve a lower misfit.

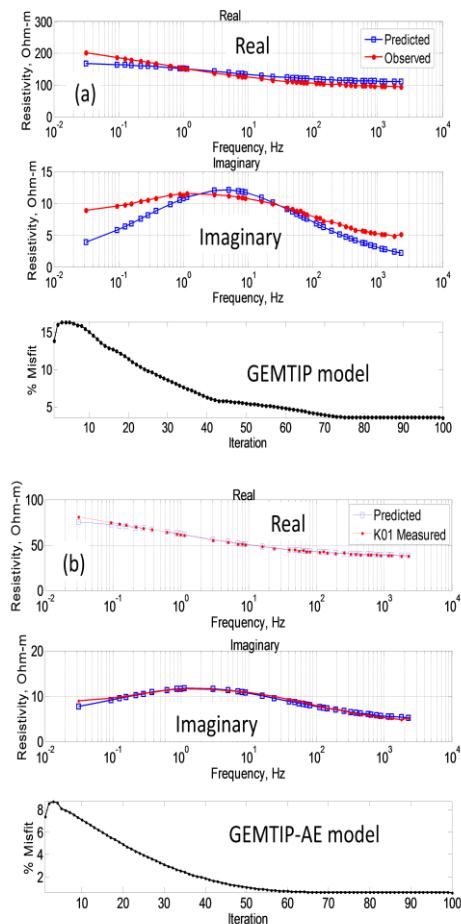


Figure 6. Observed real (top panels) and imaginary (middle panels) CR spectra (red lines and dots) for the QMP sample, with the GEMTIP-derived CR spectra (blue lines and dots) obtained using (a) a GEMTIP model with spherical grains, and (b) a GEMTIP model with elliptical grains. The misfit for each model is shown in bottom panels.

As another example, we consider an organic rich shale source rock from the Haynesville formation in Utah (Figure 7). QEMScan analysis of the sample was able to define the composition, and quantify the pyrite grain size between 0.01 mm and 0.5 mm radius (Figure 8). The pyrite fraction volume was estimated at 3.7%, and the pore volume was 1.5%. Again, the CR spectra of the sample was measured, and subsequently inverted for the pyrite fraction volume (Table 2). We inverted observed CR spectra for the desired GEMTIP parameters. We observe very good agreement between the known fraction volume (3.7%) and that recovered from the GEMTIP inversion (3.5%) (Figure 9).

Laboratory-based GEMTIP analysis of spectral IP data



Figure 7. Organic rich shale source rock sample from the Haynesville formation, Utah.

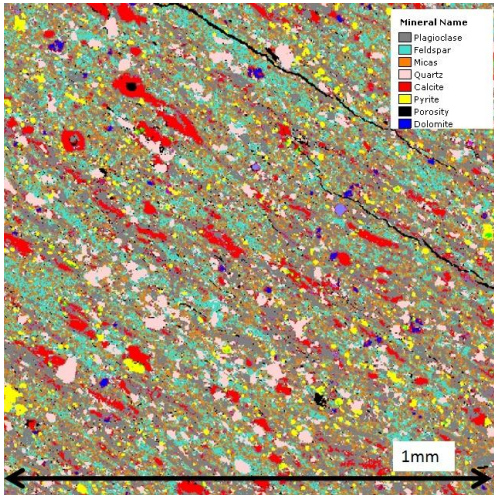


Figure 8. QEMScan analysis of the shale sample, where the cross section is parallel to the bedding plane. The sample contains 36% plagioclase, 22% feldspar, 19% mica, 11% quartz, 3.4% pyrite, and 3% calcite.

Variable	Known value	Recovered value
ρ_{matrix}	120 Ω m	-
C	-	0.33
α	-	0.40
f_{pyrite}	3.5%	3.7%

Table 2. Recovered GEMTIP inversion parameters for the shale sample.

Conclusions

In this paper, we have reviewed the use of GEMTIP for mineral discrimination, and demonstrated the ability to recover mineralogical properties from CR spectra. We are

continuing this work as part of AMIRA International project P1058, where we are analyzing samples from numerous world class mineral deposits. We are also applying GEMTIP to 3D IP inversion, to enabled EM data to be inverted for mineralogical properties.

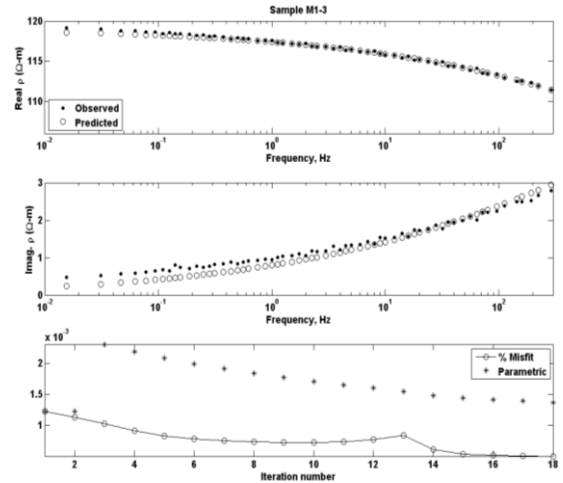


Figure 9. GEMTIP inversion of complex resistivity data measured for the shale sample.

Acknowledgements

The initial research presented in this paper was conducted at the University of Utah from 2004 to 2007 with funding from the National Energy Technology Laboratory of the U.S. Department of Energy (DOE) under contract DE-FC26-04NT42081. The research was continued from 2007 to 2010 under auspices of the University of Utah's Consortium for Electromagnetic Modeling and Inversion (CEMI). This research is continuing through TechnoImaging and AMIRA International project P1058 Spectral IP for 3D mineral discrimination, and is currently supported by Abitibi Geophysique, Anglo American, Barrick Gold, BHP Billiton, First Quantum Minerals, Geophysical Resources and Services, Khumsup, Teck Resources, Quantec Geoscience and Zonge International. This paper is published with the approval of TechnoImaging and the AMIRA P1058 sponsors. Professors Erich U. Petersen (Geology and Geophysics) and Chen-Luh Lin (Metallurgical Engineering), and CEMI graduates Abraham Edmond (M.Sc., 2007), Sam Buist (M.Sc., 2009), Charles (Roo) Philips (M.Sc., 2010), and Lei Fu (M.Sc., 2011), are acknowledged for their contributions to the results presented in this paper. Thanks are also extended to Scott Urquhart, Emmett Van Reed and Anna Szidarovsky of Zonge International Inc., for their assistance with the CR measurements presented in this paper, and for many fruitful discussions.

EDITED REFERENCES

Note: This reference list is a copy-edited version of the reference list submitted by the author. Reference lists for the 2012 SEG Technical Program Expanded Abstracts have been copy edited so that references provided with the online metadata for each paper will achieve a high degree of linking to cited sources that appear on the Web.

REFERENCES

- Burtman, V., A. V. Gribenko, and M. S. Zhdanov, 2010, Advances in experimental research of induced polarization effect in reservoir rocks: 80th Annual International Meeting, SEG, Expanded Abstracts, 2475–2479.
- Burtman, V., M. Endo, M. S. Zhdanov, and T. Ingeman-Nielsen, 2011, High-frequency induced polarization measurements of hydrocarbon-bearing rocks: 81st Annual International Meeting, SEG, Expanded Abstracts, 677–681.
- Emond, A. M., M. S. Zhdanov, and E. U. Petersen, 2006, Electromagnetic modeling based on the rock physics description of the true complexity of rocks: Applications to study of the IP effect in porphyry copper deposits: 76th Annual International Meeting, SEG, Expanded Abstracts, 1313–1317.
- Luo, Y and G. Zhang, 1998, Theory and application of spectral induced polarization: SEG.
- Marshall, D. J., and T. R. Madden, 1959, Induced polarization, a study of its causes: *Geophysics*, **24**, 790–816.
- Pelton, W. H., S. H. Ward, P. G. Hallof, W. R. Sill, and P. H. Nelson, 1978, Mineral discrimination and removal of inductive coupling with multifrequency IP: *Geophysics*, **43**, 588–609.
- Wait, J. R., 1959, *Overvoltage research and geophysical applications*: Pergamon Press.
- Wait, J. R., 1983, *Geoelectromagnetism*: Permagon.
- Zhdanov, M. S., 2002, *Geophysical inverse theory and regularization problems*: Elsevier.
- Zhdanov, M. S., 2008, Generalized effective-medium theory of induced polarization: *Geophysics*, **73**, no. 5, F197–F211.
- Zhdanov, M. S., and V. Burtman, 2009, Induced polarization in hydrocarbon-saturated sands and sandstones: Experimental study and general effective medium modeling: 79th Annual International Meeting, SEG, Expanded Abstracts, 774–778.
- Zhdanov, M. S., A. Gribenko, V. Burtman, and V. I. Dmitriev, 2008, Anisotropy of induced polarization in the context of the generalized effective-medium theory: 78th Annual International Meeting, SEG, Expanded Abstracts, 677–681.